Five Years of GPM Observations Reveal Land Surface Response to Precipitation

S. Joseph Munchak (Code 612, NASA/GSFC), Sarah Ringerud (Code 612, NASA/GSFC/UMD), Ludovic Brucker (Code 615, NASA/GSFC/USRA) Yalei You (UMD/ESSIC), Iris de Gelis (CLS, Brest, France), and Catherine Prigent (LERME, Paris, France)

Change in 10 GHz Emissivity Due to Rainfall

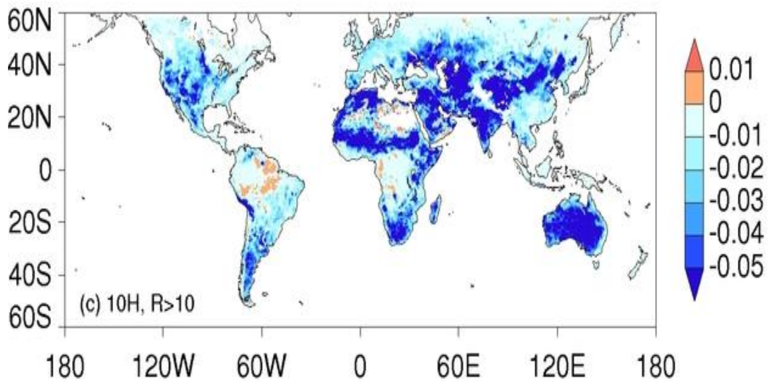

Change in K_u Backscatter Due to Rainfall (dB)

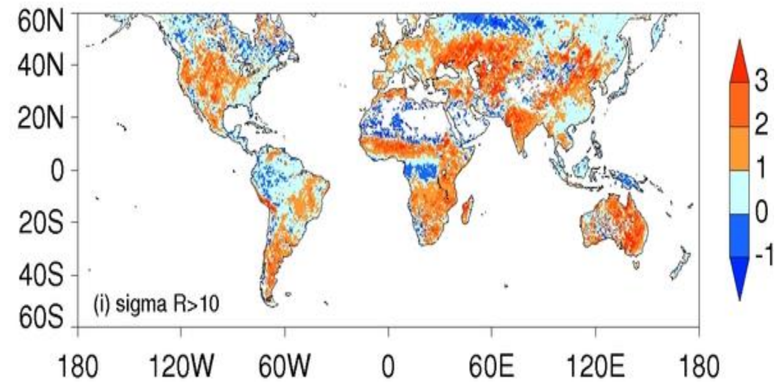

Change in 89 GHz Emissivity Due to Snowfall

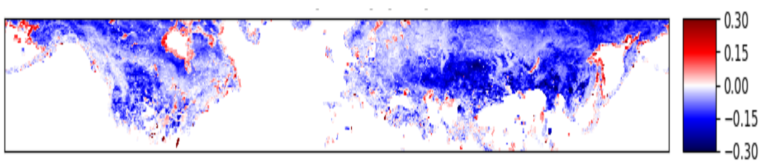

Change in K_a Backscatter Due to Snowfall (dB)

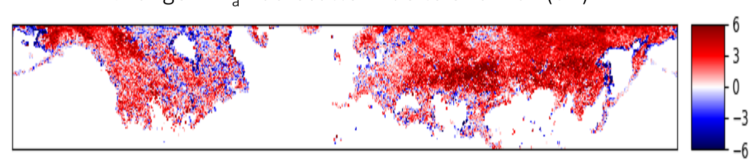

Using a 1DVAR retrieval algorithm, we examined 5 years of GPM data for sensitivity to accumulated rain and snow. Our analysis revealed significant correlation to accumulated rain at the lower frequencies in many regions and significant correlation to snowpack at the higher frequencies, showing the potential use of passive/active microwave observations for monitoring accumulated as well as falling precipitation.

Name: S. Joseph Munchak, NASA/GSFC, Code 612
E-mail: s.j.munchak@nasa.gov
Phone: 301-286-2392

References:
Publication:
S. J. Munchak, S. Ringerud, L. Brucker, Y. You, I. de Gelis and C. Prigent, "An Active–Passive Microwave Land Surface Database From GPM," in IEEE Transactions on Geoscience and Remote Sensing, vol. 58, no. 9, pp. 6224-6242, Sept. 2020, doi: 10.1109/TGRS.2020.2975477.

Dataset (open access):
S. J. Munchak, S. Ringerud, L. Brucker, Y. You, I. de Gelis and C. Prigent, "An Active–Passive Microwave Land Surface Classification From GPM," IEEE Dataport, 2019, doi: 10.21227/fypd-zj65

Data Sources: NASA GPM GMI Level 1C Intercalibrated Brightness Temperature V05A, NASA GPM DPR Level 2 Surface Backscatter Cross-section V06A, NASA GPM IMERG Gridded 30-Minute Precipitation V05A, NASA MERRA-2 3-Hourly Instantaneous Pressure-Level Assimilation Assimilated Meteorological Fields V5.12.4, NASA MERRA-2 2D 1-Hourly Instantaneous Single-Level Assimilation Single-Level Diagnostics V5.12.4, NASA MERRA-2 2D 1-Hourly Land Surface Diagnostics V5.12.4

Technical Description of Figures:
Graphic 1 (top and center right): The difference in emissivity at 10.65 GHz horizontal polarization (left) and Ku-band backscatter cross-section (right) between observations with > 10mm of rainfall in the previous 24-hour period and observations with no rainfall in the previous 24-hour period (rainfall from IMERG). Most regions show a decrease in emissivity and increase in backscatter due to an increase in soil moisture.

Graphic 2 (bottom row): The difference in emissivity at 89 GHz horizontal polarization (left) and Ka-band backscatter cross-section (right) between observations with 10-100mm of snow water equivalent and observations with < 1mm snow water equivalent (SWE from MERRA-2). Although the change in emissivity is quite variable regionally, the response at Ka band is more uniform, showcasing the potential use of this measurement for monitoring shallow snowpacks.

Scientific significance, societal relevance, and relationships to future missions: Although the original purpose of this work was to develop databases to improve the characterization and classification of surface properties in the GPM Level 2 precipitation algorithms, many additional applications are enabled by this dataset. For example, the response of the surface to accumulated rain and snow is highlighted on the previous slide, and these relationships are already being used by coauthor Yalei You to develop a multisatellite precipitation retrieval based on the change in emissivity. This method has the advantage of capturing short-lived or rapidly developing precipitation events that may be missed in between overpasses of microwave sensors. In addition, CRTM developers have inquired about the use of the GMI emissivity atlas in order to evaluate its utility in NWP data assimilation systems. Finally, the sensitivity of the Ka-band backscatter may prove to be complementary to passive microwave and SAR methods for observing a wide spectrum of snowpacks in a future SWE mission.

Deep Blue Aerosol Layer Height from VIIRS and OMPS-NM

Jaehwa Lee[2,1], N. Christina Hsu[1], and others, [1]Code 613, NASA/GSFC and [2]UMD/ESSIC

Wildfire Smoke Observed by VIIRS

Retrieved Aerosol Layer Height

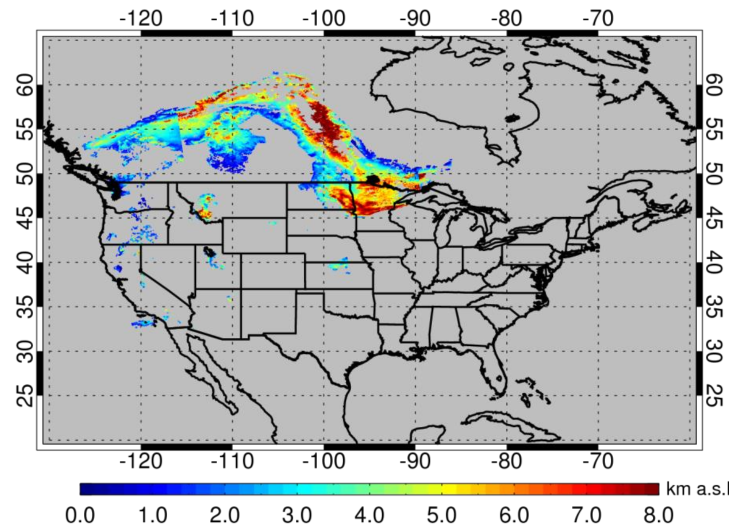

An operation-ready Aerosol Single-scattering albedo and Height Estimation (ASHE) algorithm has been implemented in the VIIRS Deep Blue aerosol algorithm suite to provide the height of absorbing aerosols from synergistic use of VIIRS and OMPS, both onboard the S-NPP satellite. With extensive spatial coverage, the data set can contribute to better understanding of the effects of aerosol layer height on aerosol radiative effects, long-range transport, and surface air quality. The data product will be available as part of the Version 2 VIIRS Deep Blue products in the near future.

Name: Jaehwa Lee, NASA/GSFC, Code 613 and UMD/ESSIC
E-mail: jaehwa.lee@nasa.gov
Phone: 301-614-6407

References:

Lee, J., N. C. Hsu, A. M. Sayer, C. J. Seftor, and W. V. Kim (in press), Aerosol layer height with enhanced spectral coverage achieved by synergy between VIIRS and OMPS-NM measurements, *IEEE Geoscience and Remote Sensing Letters*, https://doi.org/10.1109/LGRS.2020.2992099.

Lee, J., N. C. Hsu, C. Bettenhausen, A. M. Sayer, C. J. Seftor, and M.-J. Jeong (2015), Retrieving the height of smoke and dust aerosols by synergistic use of VIIRS, OMPS, and CALIOP observations, *Journal of Geophysical Research: Atmospheres*, **120**, 8372–8388, https://doi.org/10.1002/2015JD023567.

Jeong, M.-J., and N. C. Hsu (2008), Retrievals of aerosol single-scattering albedo and effective aerosol layer height for biomass-burning smoke: Synergy derived from 'A-Train' sensors, Geophysical Research Letters, 35, L24801, https://doi.org/10.1029/2008GL036279.

Data Sources: VIIRS Deep Blue aerosol data used in this study are available at https://earthdata.nasa.gov/search?q=viirs+deep+blue; OMPS L1B data at https://earthdata.nasa.gov/search?q=omps+l1b. This research was funded by NASA's Terra, Aqua, and Suomi NPP program.

Technical Description of Figures:
Graphic: ASHE algorithm, as part of Deep Blue aerosol algorithm suite, simultaneously retrieves the height and single scattering albedo (SSA) of absorbing aerosols, such as biomass burning smoke and mineral dust, using co-located 412 nm top-of-atmosphere reflectance from VIIRS and ultraviolet aerosol index from OMPS-NM. Figures show an example of ASHE applied to a North American wildfire smoke event observed on 10 August 2018 from Suomi NPP satellite. The smoke layers across the continent mainly originated from multiple fire sources in the mountainous regions of British Columbia, Canada, and persisted for weeks. The peak AOD at 550 nm of the smoke layers was higher than 3.0 over vast areas. Retrieved aerosol layer height (ALH) from ASHE suggests that significant portions of the smoke plumes were injected into the free troposphere (ALH > 3–8 km), enabling long-range transport stretching thousands of kilometers. Validation of the ALH product over North America against CALIOP during peak burning seasons from 2012-2018 (not shown) resulted in 61% (90%) of data falling within $\pm$1 km ($\pm$1.5 km) of those from CALIOP, indicating the robustness of the algorithm.

Scientific significance, societal relevance, and relationships to future missions: Since the interactions between aerosols, radiation, clouds, and precipitation, which have myriad implications for Earth's climate system, take place in 3-D space, information on the vertical structure of aerosols (in addition to their horizontal distribution) is essential for better quantification of the radiative effects of aerosols. Thus, retrievals of the height information from satellite sensors have been of great interest. CALIOP and MISR missions have successfully served the scientific community on this matter. However, with swath widths of 70 m for CALIOP and 360 km for MISR, spatial coverages of those instruments are somewhat limited. The new data product from synergistic use of VIIRS and OMPS can thus complement the existing data sets. This synergy can continue with the current JPSS mission (continued VIIRS and OMPS instruments) and planned PACE mission (OCI instrument equipped with required spectral bands in a single sensor).

GEOS GMI-based Climatology of Diurnal Variability in Stratospheric Ozone to Reduce Uncertainty in Multi-Satellite Data Records

Stacey Frith (Code 614, NASA/GSFC and SSAI), P. K. Bhartia (NASA/GSFC), Luke Oman (NASA/GFSC), Natalya Kramarova (NASA/GFSC), Richard McPeters (NASA/GFSC), Gordon Labow (NASA/GFSC and SSAI)

Diurnal Ozone Variability is strongest at polar latitudes in summer; > 10% daily variability in the stratosphere

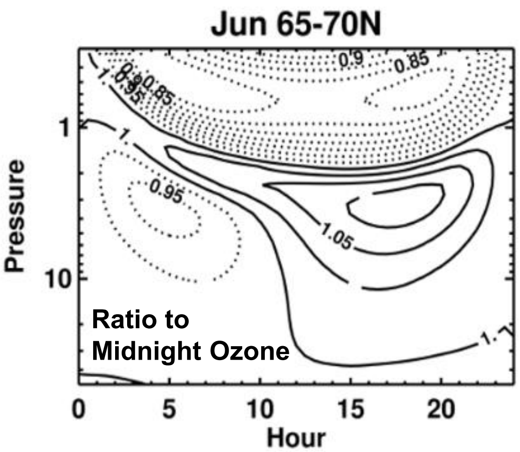

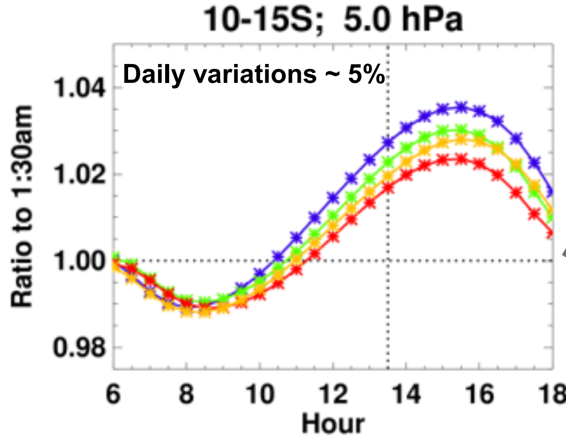

Diurnal signals are smaller at low and mid-latitudes, but they still play a significant role in data analysis, as seen in the SBUV ozone time series comparisons on the right.

10°-15°S zonal mean ozone anomalies [%], 6.39-4.03 hPa

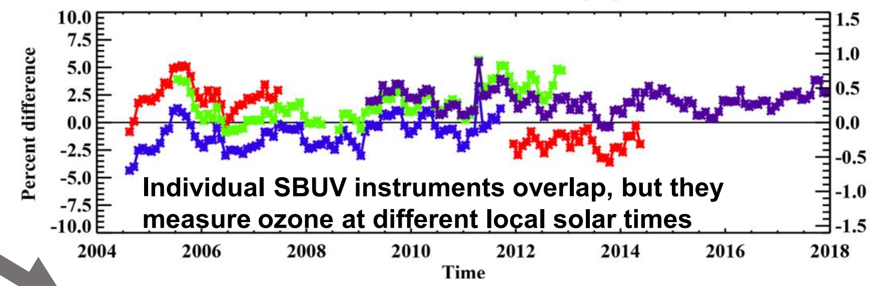

Ozone anomalies adjusted to common time (13:30)

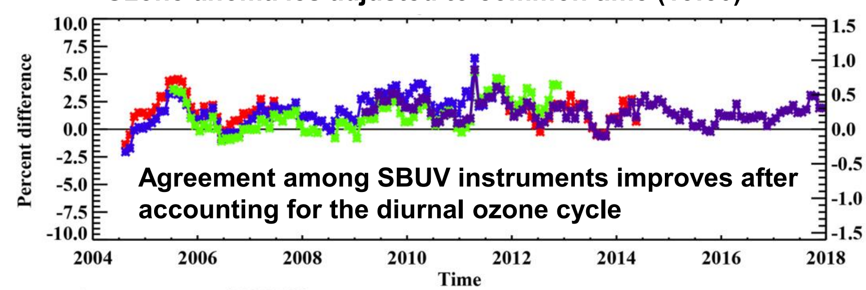

Mean = 16 DU; ___NOAA16, ___NOAA17, ___NOAA18, ___NOAA19

Observational studies of stratospheric ozone often involve data from multiple instruments measuring at different times of day. Ozone diurnal variability is largest in the mesosphere, and the smaller stratospheric signal was often ignored because a full characterization of the diurnal cycle was not available. We present a climatological representation of diurnal variations in ozone, based on NASA GSFC's GEOS-GMI model, for use in a variety of data analysis tasks.

Name: Stacey M. Frith, NASA/GSFC, Code 614 and SSAI
E-mail: Stacey.M.Frith@nasa.gov
Phone: 301-614-5984

References:

Frith, S. M., Bhartia, P. K., Oman, L. D., Kramarova, N. A., McPeters, R. D., and Labow, G. J.: Model-based climatology of diurnal variability in stratospheric ozone as a data analysis tool, Atmospheric Measurement Techniques, 13, 2733–2749, https://doi.org/10.5194/amt-13-2733-2020, 2020.

Data Sources:

The diurnal climatology presented in this work is based on output from the NASA GMAO Version 5 GEOS general circulation model, GEOS-5 (Molod et al., 2015), coupled with the NASA Global Modeling Initiative (GMI) chemistry package (Strahan et al., 2007; Oman et al., 2013; Nielsen et al., 2017), known as GEOS-GMI. The GEOS-GMI diurnal ozone climatology is stored as a NetCDF file and is available for download on our local NASA Goddard Code 614 TOMS access site https://acd-ext.gsfc.nasa.gov/anonftp/toms/ (NASA Goddard Atmospheric Chemistry and Dynamics (Code 614) Scientific/Technical Information, 2020) under subdirectory GDOC_diurnal. Also available from this site are the SBUV/2 data (subdirectory sbuv) and OMPS NP data (subdirectory omps_np). These data are also accessible via links from the Merged Ozone Data Set (MOD) website at https://acd-ext.gsfc.nasa.gov/Data_services/merged/instruments.html (NASA Goddard, 2020). Thought not shown here, several additional sources of NASA data are used in the referenced paper. OMPS LP and NP data as well as UARS and Aura MLS data are archived at the NASA Goddard Earth Sciences Data and Information Services Center (GES-DISC) (https://disc.gsfc.nasa.gov, NASA Goddard Earth Sciences Data and Information Services Center, 2019). SAGE III/ISS data are available from the NASA Langley Atmospheric Science Data Center (ASDC; https://eosweb.larc.nasa.gov/project/sageiii-iss/sageiii-iss_table, NASA Langley Atmospheric Science Data Center, 2019). Additional model output from the current GEOS-GMI simulation is available for collaborators upon request (Luke D. Oman; luke.d.oman@nasa.gov). References listed in this section can be found within the above referenced paper.

Technical Description of Figures:

Graphic 1 (left): This figure shows climatological ozone variability as a function of hour of day and pressure for the month of June in the zonal band 65-70°N, near the polar day boundary. The ozone value at each hour is expressed relative to the ozone value at midnight, in units of percent. Diurnal ozone variability is largest in the stratosphere at the polar day boundary. The climatology, based on the NASA Goddard Code 614/GMAO GEOS-GMI model, shows a pattern of low ozone in the morning and high ozone in the afternoon, consistent with other model- and observation-based analyses of the ozone diurnal cycle.

Graphic 2 (center): This figure shows the mean diurnal ozone cycle in the southern hemisphere subtropics at 5 hPa. Here the signal is much smaller, but with the same hourly pattern of lower ozone in the morning and higher ozone in the afternoon. The four lines show the diurnal ozone variation for four seasons. Although these variations are small, improved satellite measurements make these signals relevant to data analysis.

Graphic 3 (right): The NASA/NOAA SBUV series of instruments have flown on ten satellite platforms that combined cover the time period from early 1970 to the present, with continuous coverage since late 1978. To study long-term ozone in the atmosphere, we combine these records to construct a single time series for analysis. In doing so we must ensure the stability of each instrument and consistency from instrument to instrument. However, different SBUV satellite platforms operated from different orbits, such that measurements were taken at different times of day. This figure demonstrates how using the diurnal ozone climatology to account for the difference in measurement time can reduce apparent differences in the data records that might otherwise be mistaken for calibration or instrument errors.

Scientific significance, societal relevance, and relationships to future missions: The primary goal of this work was to further our analysis of long-term trends in stratospheric ozone and our understanding of the chemical composition of the stratosphere. The climatology produced in this study can be used to support any number of instrument validation studies, modeling efforts and long-term constituent analyses. The Clean Air Act Amendments of 1977, Public Law 95-95, mandates that NASA and other key agencies submit biennial reports to Congress and EPA on the state of our knowledge of the upper atmosphere, particularly the stratosphere.